Anode Baking Furnaces – Wear of Applied Refractories

T. Tonnesen, R. Telle

Refractory linings of anode baking furnaces suffer severe corrosion during operation. The service life is therefore in relation to the construction of the flue channels and walls, operation procedures of the loading and de-loading process, firing conditions, choice of the used anode raw materials, used coke for packing and recycled anode butts. The refractory lifetime is mainly influenced by corrosive attack on the flue wall refractories and occurring creep at the bottom of the walls. In principle two type furnace technologies are available for the baking process of anodes. Open top ring pit furnaces reveal a horizontal gas flow through flue walls. Pre-heated gas flows along a labyrinth of tie bricks. Closed ring pit furnaces have a vertical gas flow through the flue walls. In these post mortem studies wear and corrosion behaviour of applied refractories was observed in regard to the different furnace types. The different atmospheres and firing conditions lead to microstructural changes with different reaction zones. These are worked out by means of SEM, EDS and XRD. At the hot face a decrease in alumina and silica is significant for the examined bricks. Due to condensation and precipitation of alkaline compounds the high temperature properties have been examined in particular. Differences in the operation of the furnace are recognized for the refractories since phase formation due to volatile compounds such as ZnO, NiO and V_2O_5 were just found for the open top ring pit furnace.

1 Introduction

In principle two type furnace technologies are available for the baking process of anodes.

Thorsten Tonnesen
Rainer Telle
RWTH Aachen University
Institut für Gesteinshüttenkunde
Aachen, Germany

Corresponding author: T. Tonnesen
E-mail: tonnesen@ghi.rwth-aachen.de

Keywords: anode baking process, top ring pit furnace, wear, refractories

Open top ring pit furnaces reveal a horizontal gas flow through flue walls. Pre-heated gas flows along a labyrinth of tie bricks. Closed ring pit furnaces have a vertical gas flow through the flue walls (Figs. 1 and 2) [1].

The design and operation of a ring pit furnace is dependant on an optimized temperature distribution, low energy consumption and long refractory lifetimes [2]. Anodes are usually produced by pressing a mixture of pet coke, recycling anode butts and bonding pit. The amount of the recycling anode butts is between 5 and 25 %. During aluminium electrolysis the anode butts incorporate sodium and fluorine which are released during the baking process. Nevertheless these impurities lead to corrosion of the flue wall and tie bricks during operation of anode baking furnaces. But also other factors lead to a degradation of the applied refractories. The gas flow through the channels is mainly influenced by the construction of the flue walls, the bricks and the labyrinth of tie bricks [3].

The following wear mechanisms are active for the tie bricks in general. Containing sodium, potassium and fluorine of the anodes is released due to evaporation at the hot face near the stacked anodes. Volatile alkaline compounds diffuse via vapour phase and porosity across the brick. Condensation at the cold face results in Na_2O and K_2O contamination along the brick. Fluorine is localized at the hot face of the bricks as well as sulphur. Diffusion of the sulphur compounds is related to the fuel. Firing of the anode baking furnaces is carried out with two fuel sources. Oil or gas burners produce about 50 % of the needed energy. Residual energy is gained from released volatiles out of the coking process of the anode bonding pitch (Fig. 3).

During furnace operation the released vapour phase from anodes and fuel react with the refractory material. Reaction products mainly are carbon-, sulphur-, alkaline- and fluorine compounds. Due to thermal expansion of the wall, anode and packing coke tie bricks and flue wall bricks are exposed to

Fig. 1 **Closed ring pit furnace for anode baking [1]**

Fig. 2 **Open top ring pit furnace for anode baking [1]**

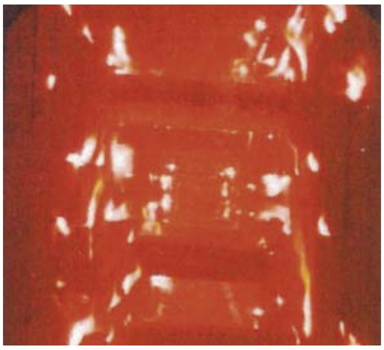

Fig. 3 Firing of volatiles [1]

Tab. 1 Chemical composition of the refractory materials

	CL As received	OP As received
Al_2O_3	50,10	52,54
SiO_2	45,35	45,84
Fe_2O_3	2,17	0,73
TiO_2	0,79	0,48
CaO	0,59	
K_2O	0,49	0,39

Tab. 2 Mineralogical composition of the refractory brick material CL

	CL As received	CL After operation
Mullite	VS	VS
Andalusite	W	W
Cristobalite	W	M
Tridymite	–	VW

VS: Very strong; M: Moderate; W: Weak; VW: Very weak

thermo-mechanical stresses. Also the blocking of expansion joints due to filling with carbon packing leads to enhanced stresses within the lining. These often results in crack formation or pinching of wall parts.

Post mortem analyses of refractories underline microstructural changes affecting different parts of the bricks. Main changes can be observed at the hot face near the anodes. Chemical wear mechanisms are reduction of SiO_2, increase of alkaline phases and fluorine and carbon deposition. Due to the reduction of SiO_2 the mullite phase is mainly reduced. Due to infiltration of alkaline compounds precipitation of alkaline rich alumosilicate phases such as leucite, nepheline and feldspars have been recognized leading to volume expansion [4]. As a consequence of occurring creep at the bottom of the flue walls an important requirement in regard to suitable refractories for anode-baking furnaces are enhanced thermo-physical properties [5, 6]. Different specifications for the lining materials have been worked out. In general the bricks should reveal a moderate porosity up to 19 %, high gas permeability, a good RUL value and low creep rates. High amounts of impurities lowering the CO resistance and the refractoriness of the bricks are also denied.

2 Experimental work

Two shaped refractory brick materials have been examined after operation in open (OP) and closed top (CL) ring pit furnaces. The main compositions of the bricks are given in Tab. 1. The focus of these studies is on the structural and microstructural changes due to the different furnace types. This was examined by means of SEM, EDS and XRD. For the SEM analysis polished specimens out of the hot face have been used.

For the brick CL, creep in compression according to DIN EN 993-9 at 1280 °C / 24 h was also determined. Finally, cycling tests between 800 °C and 1280 °C with a constant load of 0,2 MPa have been performed and the increasing contraction of the specimens have been measured. These tests have been carried out with cylindrical specimens with a diameter of 50 mm and an inner drilling of 12,5 mm in accordance to the standards for testing RUL and creep. The testing materials were exposed to 25 thermal cycles. Only the distinguished specimen CL was treated with this method in relation to a reference material with a similar composition.

3 Results

3.1 Initial microstructure

The phase composition of the brick CL as received and after operation in a closed top ring furnace is given in Tab. 2. The main phase is mullite with very strong intensity. Residual andalusite could be recognized in the bricks as received and after operation. The high temperature silica phases have changed due to operation conditions. The amount of cristobalite has increased and tridymite precipitated in very weak intensity. To demonstrate the change of the microstructure due to the operation refractory brick material, type CL and OP was examined by means of SEM and EDS in as received state and after operation as flue wall and tie brick in a closed and open top ring pit furnace for several years.

Figs. 4 and 5 show the microstructure of the bricks as received. The EDS analysis of the surface confirms the chemical analysis by XRF: A high alumina composition with > 50 mass-% alumina and 45 mass-% silica. A particular view to the microstructural details in Fig. 4 shows that the brick CL mainly reveals mullite grains as well as grains with an andalusite composition. Grog grains have a dense constitution, and a network of open porous areas is obvious. The matrix contains a silica rich glassy phase with alkaline amounts between 2 and 4 mass-%. The microstructure of the brick for open top ring pit furnace is very similar (Fig. 5). Large mullite grains are embedded in a matrix of alumosilicate composition. The glassy phase of the matrix reveals also amounts of alkaline oxides up to 5 mass-%. Gaps of several hundred microns around grog grains form an open porosity in the brick of 18 %.

3.2 Microstructure after operation

Fig. 6 gives an overview of the hot face of the CL brick. The hot face was in contact with metallurgical coke and the anodes during

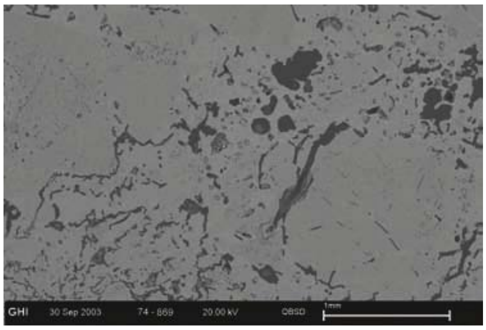

Fig. 4 Brick CL as received for use in closed anode baking furnace

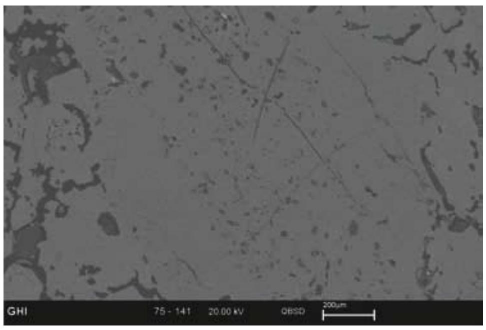

Fig. 5 Brick OP as received for use in open top anode baking furnace

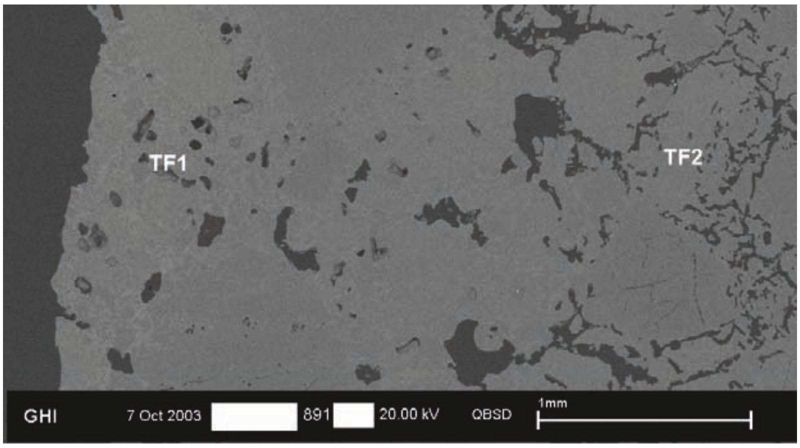

[mass-%]	Al_2O_3	SiO_2	Fe_2O_3	CaO	Na_2O	K_2O	TiO_2
TF 1	43,5	48,6	2,3	1,2	0,8	2,2	1,4
TF 2	51,7	45,9	-	-	-	1,3	1,1

Fig. 6 **SEM micrograph, brick CL after operation, overview hot face**

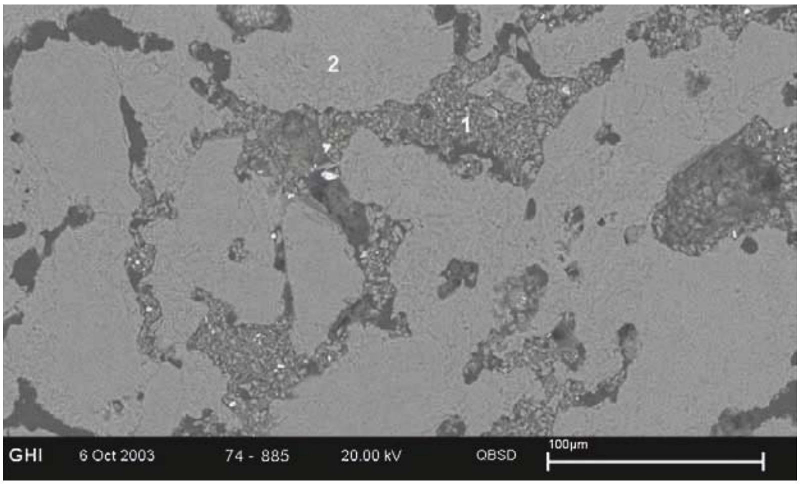

[mass-%]	Al_2O_3	SiO_2	TiO_2	Fe_2O_3
1	28,1	64,4	1,1	6,4
2	54,6	43,4	1,0	0,9

Fig. 7 **SEM micrograph, brick CL after operation, matrix near hot face**

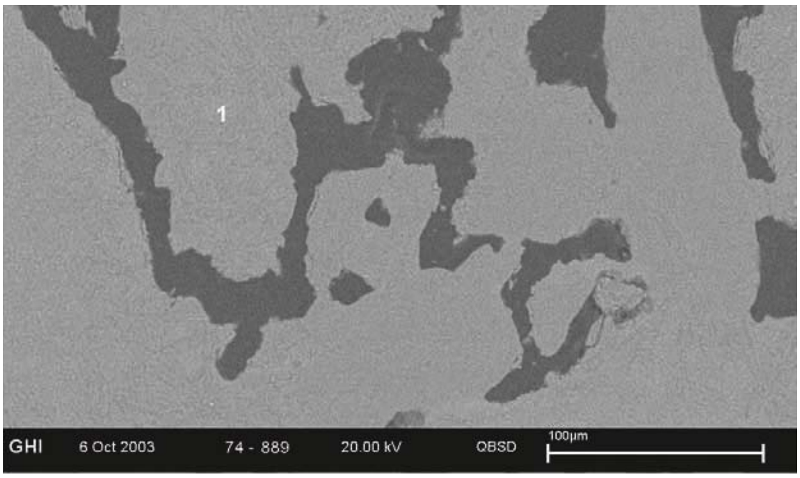

[mass-%]	Al_2O_3	SiO_2	Fe_2O_3	CaO	Na_2O	K_2O	TiO_2
1	35,8	56,4	1,5	0,7	0,9	2,7	2,1

Fig. 8 **SEM micrograph, brick CL after operation, porous matrix cold face**

operation. A densified zone of 1 mm at the hot face is obvious. Only small porosity is left. Grain growth of the former single alumosilicate and mullite grains has occurred. The chemical composition of this zone shows that the alumina content decreased. A significant increase in silica content was determined respectively. The grain boundaries are enriched with an alkali rich phase of 3 %.

The microstructure attached to the hot face reveals a regular porosity and the consistence of the grain structure. Higher alumina contents in relation to the boundary phase to coke and anodes are measured and the amount of impurities is decreased to an amount of 1,3 mass-% K_2O and 1,1 mass-% TiO_2 (Fig. 6 [TF 2]). Regarding the close-by microstructure in particular this can be confirmed. Large alumosilicate grains with a composition of 54,6 mass-% Al_2O_3, 43,5 mass-% SiO_2, 1 mass-% TiO_2 and 0,9 mass-% Fe_2O_3 are existent (Fig. 7 [2]). The porosity is filled with a silica rich phase with Fe_2O_3 enrichment up to 6,4 mass-%. Also carbon compounds could be detected within the porous structure.

Fig. 8 underlines that the shape of the porosity is still consistent at the cold face. The precipitation of silica and iron oxide rich phases within the pores does not take place in these parts of the bricks. Thus the infiltration zone is limited to small parts of the bricks. Further penetration does not occur. A constant amount of alkalis is remarkable. The sum of alkaline oxides is 3,6 mass-% whereas Na_2O was picked up during the process and K_2O amount was enhanced.

In Figs. 9 to 11 the results of the SEM examination of the brick after operation in an open top ring pit furnace (OP) are presented. Severe corrosion has taken place at the hot face of the brick. Infiltration of the grain boundaries as well as diffusion of alkaline oxides into the grains can be recognized (Fig. 9 [2–4]). The refractory constituents are mainly infiltrated leading to an elimination of the pores at the hot face. Single alumina grains are embedded by silica and alkaline rich phase. Furthermore, a phase composition of 65,3 mass-% Al_2O_3, 15 mass-% SiO_2, 10,8 mass-% Fe_2O_3, 3,5 mass-% NiO and 5,4 mass-% ZnO has been precipitated during the process (Fig. 9 [5]). A more detailed view on the reaction zone at the hot face is given in Fig. 10. It becomes obvious that sulphur compounds are also existent in this densified transition zone to the neighbouring refractory material. A layer of 60 µm has been formed at the hot face. Porosity around the grog grains is replaced by infiltrated corrosion products. Ongoing infiltration of the alkali rich phase into the refractory microstructure can be recognized. The high rate of infiltration can also be seen in Fig. 11. Relicts of the initial refractory alumina grains and reaction products at the grain boundary are visible. In the pores and at the formerly porous grain boundaries salt crystals have precipitated.

3.3 High temperature properties

Results of the thermo-physical experiments are given in Figs. 12 and 13. The creep in compression behaviour of brick CL leads to a maximum contraction of the material of 0,19 % after 25 h. The creep rate between 14 h and 25 h was determined with a low value of 0,003 %/h. The same brick was also tested in creep in compression experiments with a cycling temperature between 1280 °C and 800 °C. The 25 cycles and the resulting expansion and contraction curves are given in Fig. 13. Due to temperature and load both materials do not reach the exact initial level after each cycle. An increase in contraction can be recognized for both materials. But brick material CL shows higher rates. After 25 cycles 0,3 % contraction has been measured for brick CL. The time dependant decrease and the stronger tendency for contraction after the first cycles are different for the tested materials. The reference material stays at a constant level during the thermal cycling whereas brick CL reveals increasing contraction with time and each cycle.

4 Discussion and conclusion

These studies underline the different corrosive environments and atmospheres, which exist in the different furnace types. Initial microstructure and technological data such as bulk density and porosity are very similar for the examined bricks.

The structural analysis of the brick for the closed anode baking furnace shows that only slightly changes in the phase compositions could be determined by XRD. Mullite as main phase does not change significantly. Although residual andalusite is existent, the ongoing formation of mullite does not lead to stresses due to the transformation volume change. The changes of the applied bricks become obvious at the micro-scale. SEM and

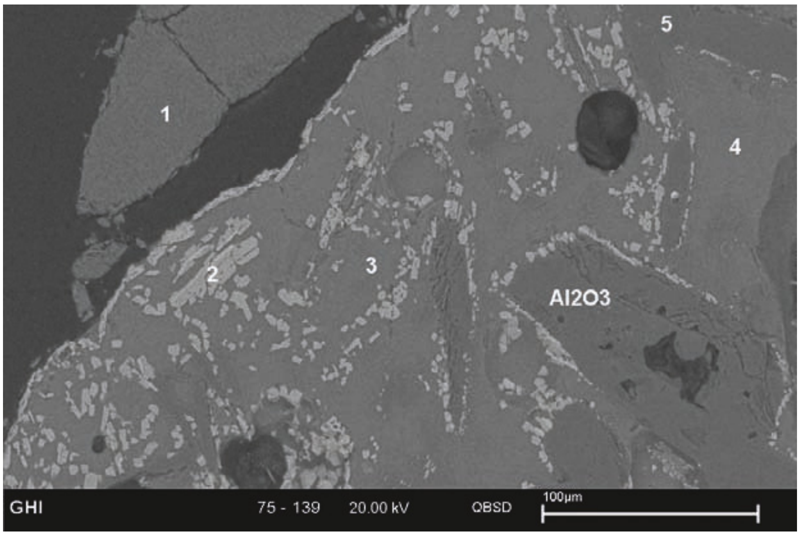

[mass-%]	Al_2O_3	SiO_2	Fe_2O_3	CaO	Na_2O	K_2O	NiO	TiO_2
1	38,3	58,9	1,5	-	-	0,3	-	-
2	24,0	53,3	8,9	-	-	3,7	2,2	7,9
3	13,5	76,8	1,5	1,4	2,0	4,8	-	-
4	13,9	73,8	4,4	-	2,4	5,6	-	-
5	65,3	15,0	10,8	-	-	-	3,5	5,4

Fig. 9 SEM micrograph, brick OP after operation, infiltration zone at the hot face

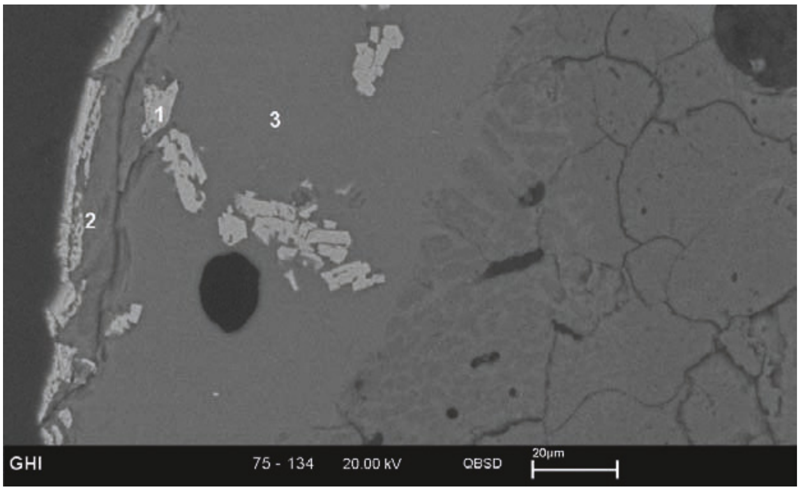

[mass-%]	Al_2O_3	SiO_2	Fe_2O_3	ZnO	Na_2O	K_2O	SO_3
1	9,3	4,1	83,4	3,2	-	-	-
2	11,3	78,8	1,2	-	2,2	6,0	0,7
3	12,2	76,9	2,3	-	2,3	5,3	0,9

Fig. 10 SEM micrograph, brick OP after operation, transition of infiltration zone to refractory, hot face

EDS examinations reveal very different corrosion mechanisms after application. The refractory material for the closed anode-baking furnace mainly shows a dense layer formation at the hot face in contact to coke and anodes. Mainly alkaline compounds are enriched up to 3 mass-% whereas K_2O shows the most increase between initial composition and analysis after operation. This enhanced level of alkaline rich phase is consistent for the whole examined microstructure. Even at the cold face 2,7 mass-% K_2O and 0,9 mass-% Na_2O are existent. Although formation of leucite, nepeheline or feldspars could not be detected by XRD, the precipitation of this alkaline rich alumosilicate phase is one of the dominant corrosion mechanisms for this type.

Also significant for almost all microstructural parts, hot face and cold face, is the de-

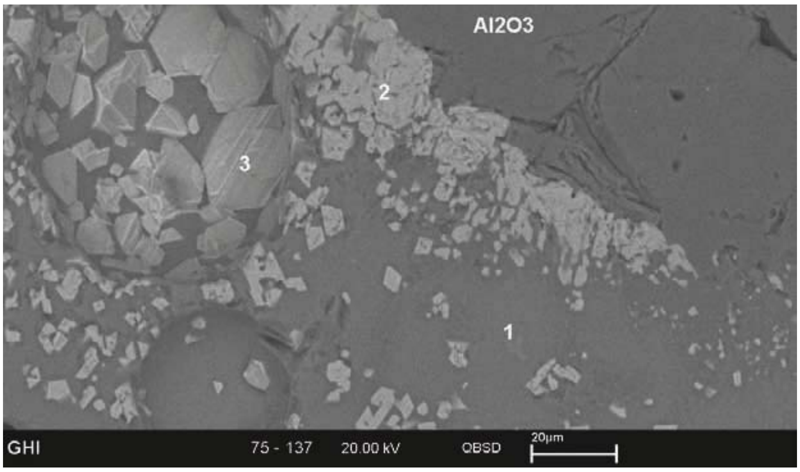

[mass-%]	Al_2O_3	SiO_2	Fe_2O_3	CaO	Na_2O	K_2O	V_2O_5	NiO	ZnO
1	13,2	74,1	2,6	1,6	2,3	4,7	1,5	-	-
2, 3	44,6	3,3	18,9	-	-	-	-	4,5	28,7

Fig. 11 SEM micrograph, OP after operation, transition of infiltration zone to refractory, hot face

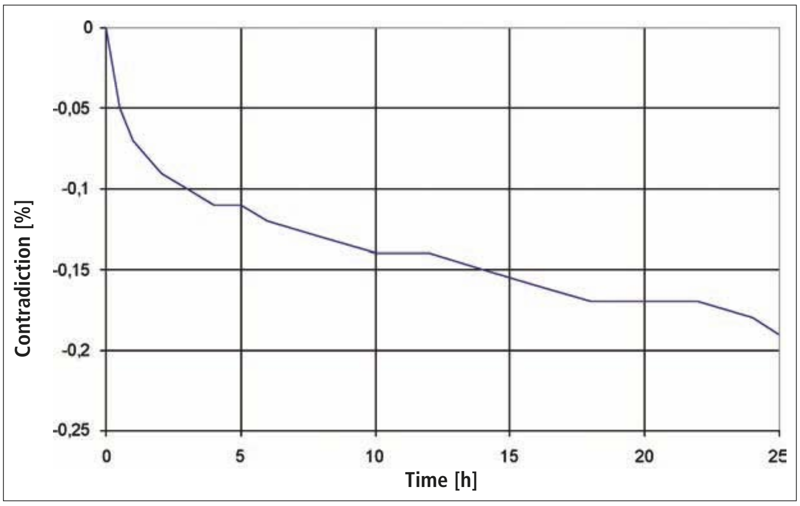

Fig. 12 Creep in compression according to DIN EN 993-9, Brick CL at 1280 °C / 25 h / 0,2 MPa

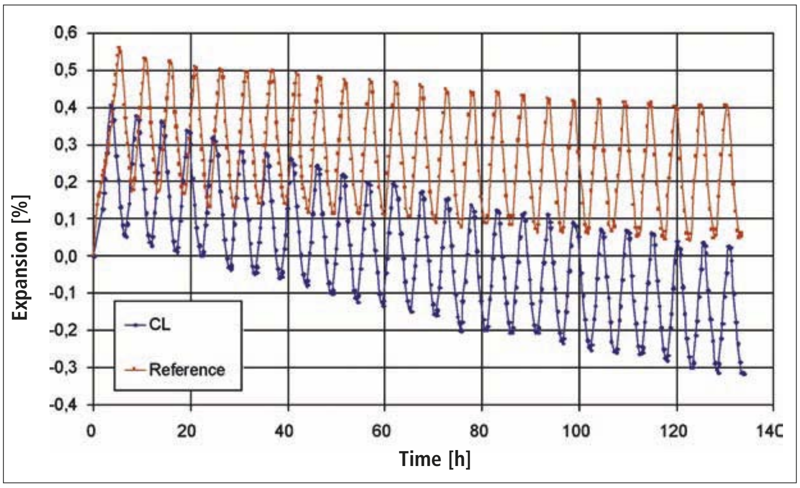

Fig. 13 Creep in compression 1280 °C – 800 °C – 1280 °C, load 0,2 MPa, brick CL and reference material

crease in the alumina content. The values scatter between 43 and 35 mass-% for the dense zone at the hot face and the matrix at the cold face, respectively. Furthermore, a mechanism common from other studies is the precipitation of carbon compounds and silica rich phases with high Fe_2O_3 content given in Fig. 4. In distance to the hot face this phase disappears and the open porous structure is mainly present at the cold face. The significant porous network formed by sintered alumosilicate and mullite grains becomes obvious and unaffected again.

Thermo-physical stability is also given in regard to the results of a single creep in compression test. The stable microstructure seems to be helpful for the mechanical stability. Low creep values after 25 h and a low creep rate of 0,003 %/h are the consequence. High amounts of Fe_2O_3 (Fig. 7 [1]) located within the porosity seem not to affect the creep behaviour of the total refractory brick. However, the long-term creep behaviour, simulated by the thermal cycling experiments with constant load, is influenced. Fig. 13 demonstrates that the brick specimen CL shows contraction starting at the fifth thermal cycle between 1280 °C and 800 °C. After 25 cycles the material has suffered a contraction of the initial expansion of 0,4 %. The increasing tendency of compression is obvious in relation to the reference refractory material.

The influence of a different furnace type and different operation conditions between closed and open top ring pit furnaces becomes clear regarding the microstructure of brick OP (Figs. 9–11). Due to different fuels for firing other compounds become dominant for the corrosion behaviour of this brick. Infiltrating species such as V_2O_5, ZnO and NiO lead to a degradation of the microstructure at the hot face. These species is missing for the specimen originating from a closed anode baking furnace. However they are part of the used fuel. The wear leads to a silica rich reaction zone with a dimension of 200 µm. Residual alumina grains are embedded. At the grain boundaries different phases are formed. On one hand dense silica rich phase with alkaline compounds of 8 – 10 mass-% precipitate. At the direct hot face also sulphur was determined (Fig. 10 [2, 3]). These examinations underline former research studies [4]. The formation of alumina rich phases with 29 mass-% ZnO, 4,5 mass-% NiO and 19 mass-% Fe_2O_3 have to be considered in regard to the used fuel for firing and the composition of coke and anodes. Refractoriness and lifetime will be affected due to the high amounts of corrosion products. The reaction mechanisms are evaporation, diffusion via vapour phase, condensation and low melting phase precipitation.

The ongoing reactions and the formation of a transition zone are remarkable and one difference of these types. At the hot face the adjacent refractory microstructure of brick CL shows porosity and scatters in the chemical load. The infiltrating species of brick OP, such as ZnO and NiO, affect the microstructure also in parts of the microstructure at the cold face. Corrosion by alkaline compounds is also effective in these parts leading to a degradation of high temperature performance.

A corrosion of the refractory bricks by infiltration of fluorine could not be confirmed by these studies. This is also related to the composition of recycling anodes. Decreasing amounts of alumina was found as a common result for both refractory materials at the hot face. The formation of low melting phases is mainly dependant on the composition of the vapour phase. Therefore enhanced wear is controlled by the infiltration of these phases and their reaction with the alumosilicate matrix. Reduced amounts of the main refractory phases are a consequence. Related changes of the thermophysical properties could be recognized. These occur on a reasonable level.

References

[1] Baking furnaces for manufactured carbon. Riedhammer GmbH, Nürnberg, Germany

[2] Becker, F.; Goede, F.: Ring pit furnaces for baking of high quality anodes – an overview. Aluminium 82 (2006) 844–853

[3] Kirschen, M.; Schwaiger, R.; Monsberger, G.: Computational fluid dynamic simulations of gas flow and heat transfer in aluminium anode baking furnaces. RHI Bull. (2006) [3] 19–23

[4] Mishra, N.; Kartik, R.; Bose, A.; Choudhuri, S.: A study of alkali attack on 42 – 45 % alumina bricks for anode baking furnace. Proc. UNITECR 2001, pp. 975–982

[5] Ghosh, B.; Sinha, R.; Chattopadhyay, A.: Alumino silicate refractories for special applications in non-ferrous metallurgy: Processing and microstructure. Proc. UNITECR 2005, pp. 652–656

[6] Tonnesen, Th.; Telle, R.: Corrosion and thermo-physical properties of refractories in closed and open top ring pit furnaces for anode baking. Proc. 52. Int. Colloquium on Refractories Aachen, 2009, in print